Analyst

Accepted Manuscript

This is an *Accepted Manuscript*, which has been through the Royal Society of Chemistry peer review process and has been accepted for publication.

Accepted Manuscripts are published online shortly after acceptance, before technical editing, formatting and proof reading. Using this free service, authors can make their results available to the community, in citable form, before we publish the edited article. We will replace this *Accepted Manuscript* with the edited and formatted *Advance Article* as soon as it is available.

You can find more information about *Accepted Manuscripts* in the Information for Authors.

Please note that technical editing may introduce minor changes to the text and/or graphics, which may alter content. The journal's standard Terms & Conditions and the Ethical guidelines still apply. In no event shall the Royal Society of Chemistry be held responsible for any errors or omissions in this *Accepted Manuscript* or any consequences arising from the use of any information it contains.

ROYAL SOCIETY OF CHEMISTRY

www.rsc.org/analyst

Oxides in silver-graphene nanocomposite: Electrochemical signatures and electrocatalytic implications.

Sajad Ahmad Bhat[a], Mudasir Ahmad Rather[a], Sarwar Ahmad Pandit[a], Pravin Popinand Ingole[b], Mohsin Ahmad Bhat[a]*

[a]*Department of Chemistry, University of Kashmir, Srinagar-190006, J&K, India.*

e-mail; mohsinch@kashmiruniversity.ac.in Fax: +91 194-2414049; Tel: +91 194 2414049.

[b]*Department of Chemistry, Indian Institute of Technology Delhi, Hauz Khas, New Delhi 110016. India.*

Abstract:

Herein we report an electrochemical approach to establish the presence of silver oxides in silver-reduced graphene oxide (Ag-rGO) nanocomposites synthesised under alkaline conditions. The recorded electrochemical signatures further supported and validated by UV-Vis spectroscopy, XRD and TEM analysis clearly establish the presence of oxide phase of silver in the nanodimensional silver present in Ag-rGO. The Ag-rGO was tested for its electrocatalytic and electrosensing activity for hydroquinone (H_2Q) and ascorbic acid (AA). The presented results establish that the electrocatalytic and electrosensing potential of the Ag-rGO for H_2Q and AA can be enhanced through electro-reduction of the oxide phase of silver in these nanocomposites. Our results prove that electrocatalytic and electroanalytic activity of electro-reduced Ag-rGO for AA are better than most of the electrode materials reported so far in the literature.

KEY WORDS: Ag/Ag_2O-rGO, Ascorbic acid, Hydroquinone, Electrooxidation, Electrocatalysis, Electroanalysis.

Analyst Accepted Manuscript

1. Introduction:

The size, shape and composition dependent electron transfer characteristics of metal nanoparticles (MNPs) and metal/metal-oxide nanoparticles (MONPs) have established them as promising entities for the design of novel electrode materials.[1-3] Immobilisation of appropriate sized/shaped MNPs/MONPs onto the host of conductive surfaces is a common approach practised by electrochemists to use/test the electrode characteristics of MNPs/MONPs. At times the novel synergism between the host and MNP/MONP characteristics has been observed to result in a significant enhancement in the catalytic and analytic performances of composites.[4-8] In view of these above cited facts and presumptions, the design of appropriately supported MNPs/MONPs hybrid materials/composites for electrosensing and electrocatalytic activities, is a fascinating and promising area of research in material electrochemistry. In the search for appropriate supporting materials for such nanocomposites, graphene and its related forms like graphene oxide(GO) and reduced graphene oxide (rGO) have emerged as promising materials for deposition of various MNPs and MONPs.[1,2,9,10] In fact the high surface area, easy to functionalize structure and good electronic conduction characteristics of graphene and rGO have opened up a cascade of opportunities for designing of novel next generation electrocatalysts.[11] The synthesis of graphene/GO immobilised silver, gold, platinum and palladium nanoparticles has been reported by several research groups.[12-16]Among metals, silver nanoparticles deposited onto graphene/rGO have been found to exhibit excellent electrocatalytic and electrosensing properties.[17, 18] Needless to mention, the electrocatalytic and electrosensing properties of nanodimensional silver composite materials are strongly sensitive to the shape, size and oxidation state of the silver. In this regard, synthesis and electrocatalytic activity of varied shaped-sized nano silver supported on rGO (Ag-rGO) has been reported by many research groups.[19-21] In most of these reports the synthesis of Ag-rGO composites has been carried out under alkaline conditions.[17,22,23] It is pertinent to mention that under basic conditions the presence of oxy-functionalities viz. hydroxyl, carboxyl, epoxy,

Analyst Accepted Manuscript

aldehydic and ketonic groups on its basal and edge planes make graphene oxide a modest reducing agent. This reducing ability of graphene oxide under alkaline conditions is well suited for reduction of Ag^+ to plasmonic silver Ag (0) and self reduction of GO to rGO.[24,25] Recently it has been reported that under strongly alkaline conditions precipitation of Ag (I) to silver oxide (Ag_2O) and silver hydroxide is more favourable and the resulting metal oxides/hydroxides better adhere to the oxide surfaces than noble metal itself.[26] Also precipitation of silver from its aqueous salt solutions in presence of strong alkali (NaOH and KOH) has been found to result in formation of Ag_2O.[27,28] In light of these above cited reports it seems that synthesis of nano sized silver under alkaline conditions on rGO must be associated with formation of oxide phase of the silver. The presence of oxide phase is expected to significantly affect the electro-catalytic and electro-sensing properties of Ag nanoparticles. Surprisingly such possibility has not been researched into by the previous works related to synthesis and electrochemical investigations on to Ag-rGO composites. Through the present work we wish to establish that silver exists both in its native and oxide form in Ag-rGO composite synthesised under alkaline conditions, and the presence of oxide phase of silver significantly alters the electrocatalytic and electrosensing activities of these composites.

2. Experimental:

2.1.Reagents and materials:

Graphite powder with particle size < 50μm, CAS# 7782-42-5 and hydrogen peroxide (30%) were obtained from E-Merck. Sulphuric acid (98%), potassium permanganate, sodium hydroxide pellets, potassium nitrate were procured from Merck India. Silver nitrate ($AgNO_3$) of AR grade was obtained from SRL chemicals. AR grade hydroquinone from SD Fine chemicals, ascorbic acid and glutaraldehyde (25%) procured from Himedia and triple distilled water as solvent were used for the presented study.

2.2.Synthesis of Ag-rGO nanocomposite:

Analyst Accepted Manuscript

Graphene oxide was synthesized from graphite powder through improved Hummer's method.[29] In a typical synthetic protocol, a 9:1 (v/v) mixture of concentrated H_2SO_4/H_3PO_4 was added to a mixture of 1.5 g of graphite powder and 9 g of $KMnO_4$. The reaction mixture was kept on stirring for 12 hours at temperature of 50 ^oC. Then after the reaction mixture was cooled to room temperature and 3-4 mL of 30% H_2O_2 were added to it to reduce the greenish coloured residual permanganate and manganese dioxide to colourless soluble manganese sulphate. Plenteous amount of triple de-ionized water was added to the reaction mixture and kept on stirring at temperature of 90 ^oC for 15 minutes. The filtrate was subjected to centrifugation; the solid material was washed several times with water and 30% HCl and finally coagulated with ether. The final product viz. graphene oxide (GO) obtained as dark brown crystalline powder was vacuum dried at room temperature and stored under inert atmosphere in a desiccator.

For the preparation of nanosized silver modified reduced graphene oxide (Ag-rGO), a reported procedure with slight modifications was followed.[22,23] Typically, 0.5 mg/mL of graphite oxide obtained from above procedure was dispersed in 100 mL of triple distilled water and ultra-sonicated for 1 hour to form yellow-brown exfoliated graphene oxide sheets (GO). The temperature of reaction mixture was raised to 60 ^oC and 44 mg of $AgNO_3$ were added slowly under constant stirring conditions. Around 15 mL of 8 M aqueous solution of NaOH was added drop-wise to the reaction mixture under stirring. The reaction mixture with continuous stirring was kept at 60 ^oC for about half an hour. The black precipitate obtained in this way (Ag-rGO) was washed several times to remove unbound silver and other impurities and finally dried under ambient conditions.

2.3.Instruments:

UV-Visible spectra were recorded on Shimadzu UV-Vis spectrophotometer (UV-1650PC) equipped with a thermostat for temperature control with accuracy of ± 0.1 ^oC. TEM analysis was carried with FEI-Technai-G 20 with a LaB6 filament, operated at 200 keV while XRD were recorded with Rigaku Miniflex 600 (Rigaku Corporation, Japan)., with source CuKa. SEM and elemental analysis

Analyst Accepted Manuscript

measurements were carried out using JEOL EDS System Instrument 6010LA operated at 15 KV. Electrochemical measurements were performed with a Metrohm Autolab potentiostat/-galvanostat (PGSTAT-100N) and the details of measurement procedures are discussed elsewhere.[30] A three electrode set-up with glassy carbon (GCE, 2 mm diameter) or GCE modified with Ag-rGO as working electrode, platinum wire as counter electrode and Ag/AgCl 3M KCl as reference electrode all from Metrohm devices, Netherlands was used for presented electrochemical investigations**.**

For the preparation of Ag-rGO modified GCE electrode, the GCE (2 mm diameter) was polished with alumina slurry 0.5~0.05 μm, followed by washing with copious amount of triple distilled water and finally with ethanol. Aqueous dispersion of the composite was prepared by dissolving 3mg of Ag-rGO per mL of water with addition of 7 μL of 25% glutaraldehyde as binder and sonicating the mixture for one hour at 25 ^{o}C.[31]Appropriate volume of the aqueous dispersion was drop casted on GCE disk, and allowed to dry under ambient conditions for 12 hours. Prior to electrochemical measurements the electroanalyte solutions were purged with argon gas for 10 minutes and kept covered with an Ar blanket during the measurements.

3. Results and Discussions:

3.1. Physico-chemical characterisation of Ag-rGO:

UV-Vis spectrum of Ag-rGO is depicted in Figure 1(A) along with inset for graphene oxide (GO). The UV-Vis spectrum of graphene oxide displays a peak at 231 nm and a hump at 293 nm which are attributed to the π-π* transitions of aromatic C=C bond and n-π* transitions of C=O bond in graphene oxide (GO), respectively.[29]The UV spectrum of Ag-rGO shows two broad bands in the range of 250-270 nm and 380-420 nm. Absorption band at 250-270 nm is attributed to the restoration of conjugation due to removal of some oxy-functionalities on reduction and band at 380-420 nm is characteristic of metallic silver surface plasmon resonance (SPR) indicating the formation of silver nanoparticles on reduced graphene oxide. The broadening of SPR band can be attributed to presence

Analyst Accepted Manuscript

of silver oxide phase of Ag NPs and presence of native silver in agglomerated form dispersed on rGO. [21, 23, 32]

The presence of nanodimensional silver on reduced graphene oxide was also confirmed from SEM and TEM analyses. Figure 1(B) and 1(C) show TEM images obtained for the synthesized composite which clearly demonstrate the presence of silver nanoparticles well dispersed on the surface of rGO. The size of silver nanoparticles was found to vary from 5 nm to 25 nm. The formation of some large sized nanoparticles with higher density can be attributed to agglomeration of silver nanostructures. The SEM images (Figure SI-1) also depicts the presence of NPs dispersed throughout the rGO surface. The elemental analysis from EDS measurements on the sample surface suggests the presence of ca. 48% of Ag along with ca. 34% of O which indicates the formation of silver oxide on rGO surface.

The XRD pattern recorded for the Ag -rGO composite synthesised for present study is depicted in Figure 1(D). The four intense peaks observed at 2θ values of 38.6^o, 44.8^o, 64.8^o, and 77.8^o can be assigned to (111), (200), (220) and (311) planes of metallic silver and confirm the presence of AgNPs in face-centred cubic phase (JCPDS file No. 04-0783).The broadened nature of XRD reflections below 25° suggests the presence of reduced graphene oxide. Moreover, the peaks observed at 34.4^o, 38.6^o and 55.8^o can be attributed to the (111), (200) and (220) diffraction planes of cubic Ag_2O with d-spacing values of 2.61 Å, 2.32 Å and 1.65 Å, respectively (JCPDS file No. 41-1104). The UV-Vis and XRD data clearly establish that in the Ag/Ag_2O-rGO composite synthesised under alkaline conditions silver is present both as native silver (Ag^0) and oxide (Ag_2O). Thus, the broad SPR bands, XRD-pattern, SEM & TEM images and EDS analysis clearly establish the presence of polydisperse nanocrystalline Ag (0)/Ag_2O aggregates dispersed on rGO.

Analyst Accepted Manuscript

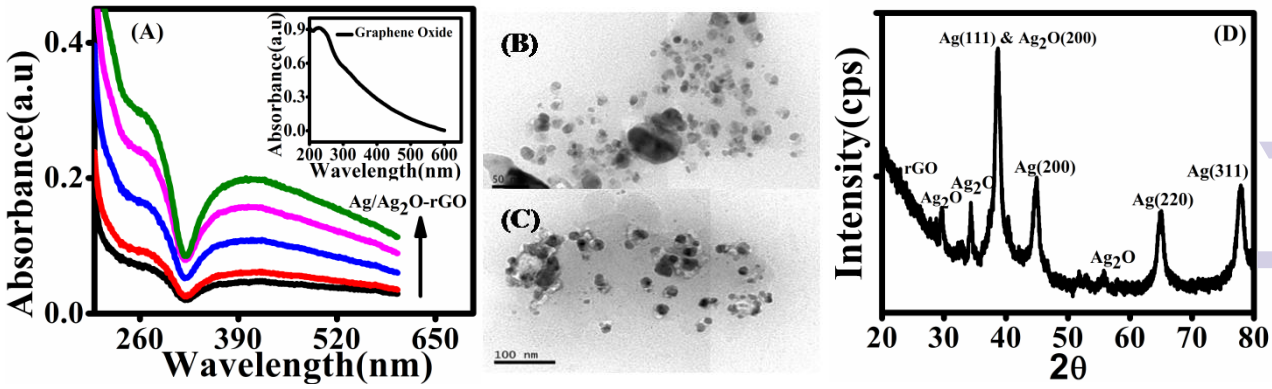

Figure 1. (A) UV-Visible spectra of silver (Ag) on rGO depicting surface plasmon resonance peak of silver and characteristic peak of C=C for reduced graphene oxide. Inset graph shows UV-Vis spectra of graphene oxide with characteristic peaks for C = C and C = O. (B & C) TEM Images of Ag -rGO nanocomposite. The images clearly depict presence of polydisperse nanoparticles in the size ranging from 5-25 nm. (D) XRD Spectra of Ag-rGO nanocomposite. The spectrum shows diffraction peaks corresponding to various phases of Ag and Ag_2O.

3.2.Electrochemical behaviour of Ag-rGO:

To explore the electrochemical behaviour of Ag -rGO synthesised for the present study, CVs of Ag -rGO modified GCE were recorded in citrate buffer of pH 4.2. The citrate buffer was used in place of phosphate buffer in view of the fact that in comparison to phosphate, citrate ions show lesser tendency to interact with Ag^+ at room temperature.[33]Figure 2 (A) and (B) depict three successive CVs recorded on Ag-rGO modified GCE at scan rate of 25 mV/s with the conditioning as well as start potential at 0.04 V with potential cycling in negative and positive directions respectively. Scanning potential in negative direction gives a broad cathodic peak (C1) around potential of -0.480 V (shown as inset of Figure 2 (A)) and an intense anodic stripping peak (A1) at 0.235 V in the reverse scan. In light of the reported electrochemical behaviour of nanophase silver[33], we attribute the presence of peak C1 to reduction of Ag_2O to Ag (0) present in Ag-rGO and peak A1 to the oxidation of Ag (0) to Ag_2O. Large anodic peak current observed in *scan 1* is probably an outcome of increase in the extent of native silver due to electro-reduction of Ag_2O when potential is scanned in negative direction. The increase in peak current associated with A1 in successive scan can be attributed to reduction of Ag_2O in the voltammetric scan beyond the potential that marks the beginning of peak A1. With conditioning and

Analyst Accepted Manuscript

start potential at 0.04 V and potential scanning in positive direction, yields CV with an anodic peak (A1) at 0.231 V and a cathodic peak (C1) at -0.480 V (Figure 2B). In the successive scans while the peak height corresponding to A1 increases with every passing scan, the reverse is the case for peak C1.

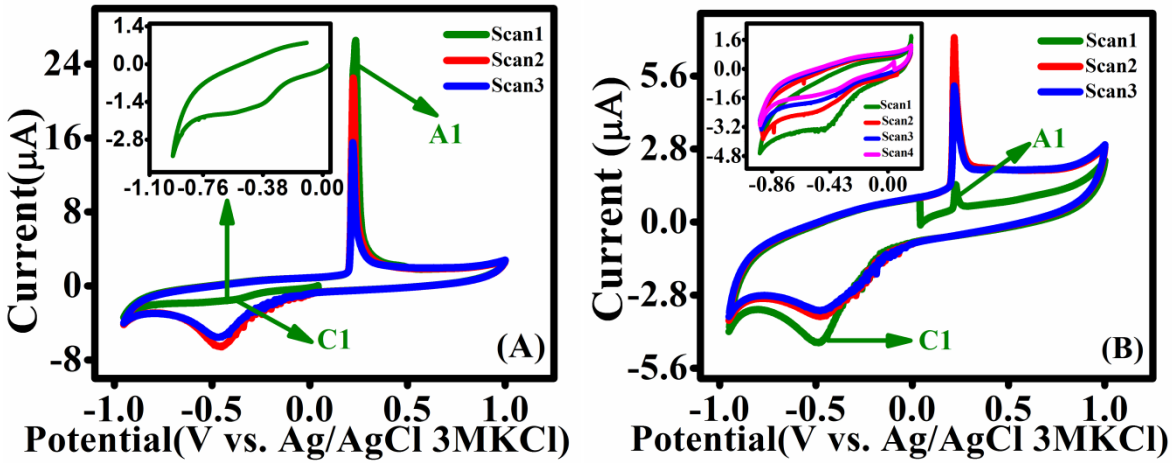

Figure 2. Three successive CVs recorded for Ag-rGO/GCE in Citrate Buffer pH 4.2 at 298 K with scan rate of 25 mV/s in cathodic (A) and anodic (B) direction respectively. The parameters are: First conditioning potential as well as start potential of 0.04 V, Potential range of -0.9 to 1.23 V. The inset in Figure 2 (A) depicts broad cathodic peak of Ag_2O observed during scan 1. The inset in Figure 2 (B) depicts four successive CVs recorded for Ag-rGO/GCE under same experimental conditions with peak reversal before oxidation of silver recorded in cathodic direction.

The position of peaks A1 and C1 on potential scale in Figures 2(A) and 2(B) matches well with those reported for oxidation of native silver and reduction of Ag_2O in similar buffered conditions.[33] These features associated with CVs depicted in Figures 2(A) and 2(B) clearly establish that in the Ag-rGO synthesized for the present work, silver exists both in its native as well as Ag_2O. The charge efficiency (CE) of the redox pair (A1-C1), defined as the ratio of area under anodic peak (Q_a corresponding to Ag to Ag^+) and that under cathodic peak (Q_c corresponding to Ag_2O to Ag) was found to be 1.2 ± 0.05. This observed value for CE also attests the presence of mixture of Ag and Ag_2O in the Ag-rGO nanocomposite.[33] As depicted in inset of Figure 2(B), CV scans with potential limits negative to position of peak A1 result in decrease of the height corresponding to peak C1. This implies that holding the composite at potentials negative to -0.5 V vs. Ag/AgCl/3M KCl results in decrease of the silver oxide content in Ag/Ag_2O-rGO composite. These above mentioned electrochemical observations and inferences commute with XRD & EDS analysis which proves the presence of Ag in native as well

Analyst Accepted Manuscript

as in oxide form on reduced graphene oxide. It is in this context that beyond this section of the MS the Ag-rGO composite synthesised for present work is referred to as Ag/Ag_2O-rGO.

Figure 3 depicts CVs recorded at changing scan rates (10 -100 mVs^{-1}) for Ag/Ag_2O-rGO modified electrode in citrate buffer solution. It clearly indicates that with increase in scan rate while the peak potential corresponding to peak C1 drifts negatively, the position of peak A1 remains unaltered on potential axes. This implies that a fast electron transfer process probably associated with desorptive stripping of the electro-active species results in anodic peak A1, and a kinetically slow heterogeneous electron transfer process is responsible for cathodic peak C1. Since peak C1 is attributed to reduction of Ag_2O, the slow kinetics of the said process as implied by Figure 3 suggests higher stability of Ag_2O phase on Ag/Ag_2O-rGO, which can be attributed to pi-accepting or electron withdrawing nature of rGO.

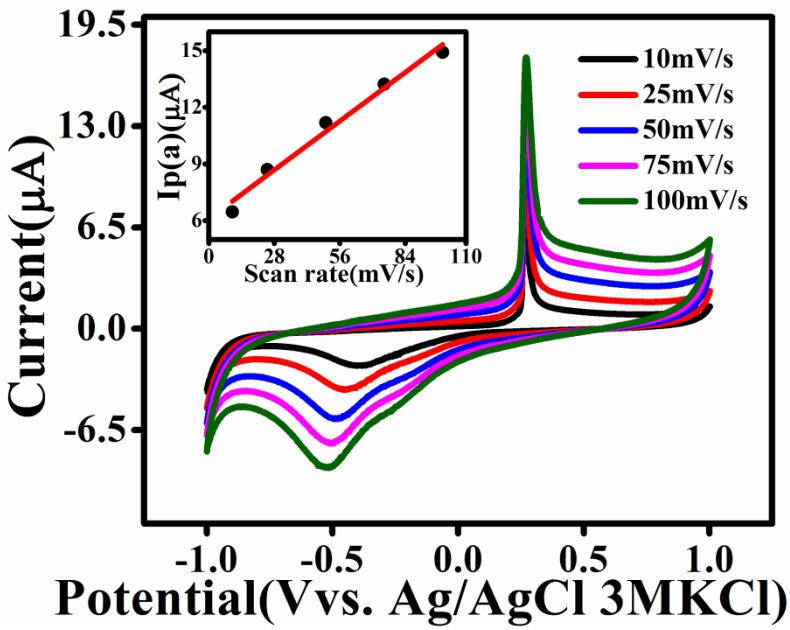

Figure 3. CVs recorded for Ag-rGO/GCE in citrate buffer of pH 4.2 at 298 K with changing scan rates (10-100 mV/s). Inset shows plot of Ip vs. scan rate (mV/s) for anodic peak and its linear fit (R^2 = 0.99) with slope 0.092.

The data depicted in Figure 3 was processed for estimation of the surface concentration (Γ) of Ag on Ag- rGO composite.[21] 'Γ' corresponding to Ag was determined from the slope of the I_p vs. scan rate (v) plot (inset Figure 3) for peak A1 in the CVs depicted in Figure 3 following equation 1[21]:

Analyst Accepted Manuscript

$$I_p = \frac{n^2 F^2 A \Gamma v}{4RT} \quad (1)$$

Where n represents number of electrons involved in the electrode reaction, A is the geometric surface area of the electrode (0.0314 cm^2), Γ (mol/cm^2) is the surface coverage, rest of the terms R, T and F have their respective meanings. The $I_{p\,(a)}$vs. v data was observed to fit a linear equation (R^2= 0.99) with slope 0.092.The effective electroactive surface area of the Ag/Ag_2O-rGO modified glassy carbon electrode was estimated by chronocoulometry using hydroquinone with diffusion coefficient 8.8 × 10^{-6} cm^2s^{-1} [34] as a redox probe. With known value of slope corresponding to $I_{p\,(a)}$vs. v plot, the surface concentration of native Ag in Ag/Ag_2O-rGO composite was found to be 3.12 × 10^{-6} mol/cm^2. The estimated value is almost an order of magnitude lower than that reported for the Ag/Ag_2O-rGO composite synthesised under similar conditions.[23]

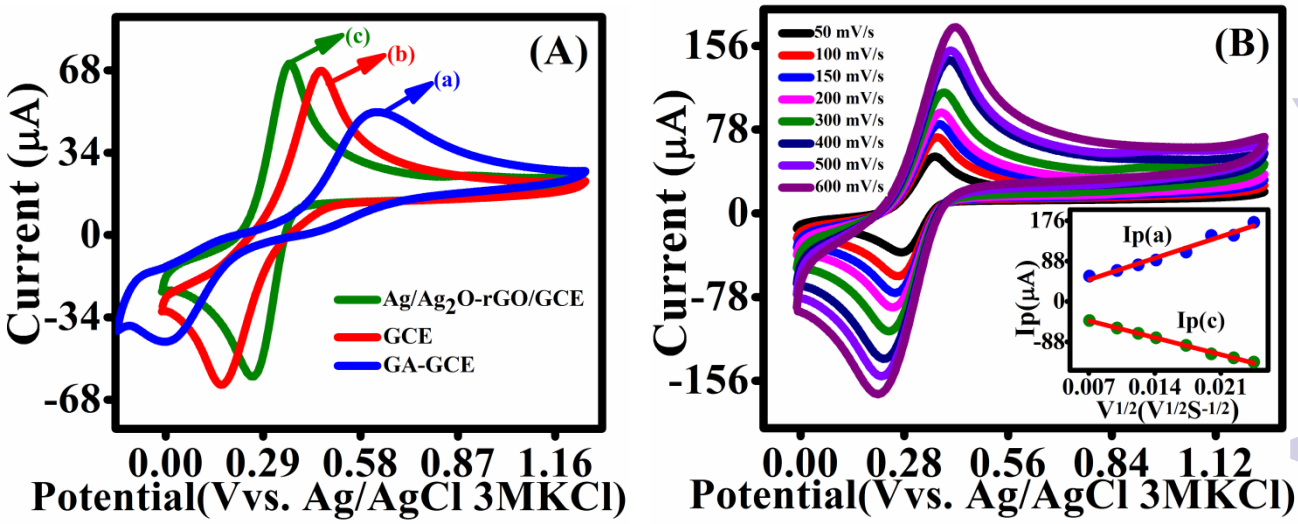

Figure 4. (A) CVs recorded for 4 mM Hydroquinone (H_2Q) in 0.1N KNO_3(a) Blue on GA-GCE (b) Red on GCE (c) Green on Ag/Ag_2O-rGO/GCE, at 298 K with scan rate of 100 mV/s. (B) CVs recorded on Ag/Ag_2O-rGO/GCE for 4 mM Hydroquinone(H_2Q) in 0.1N KNO_3 at 298 K with changing scan rates (50-600 mV/s). Inset shows plot between Ip vs. $v^{1/2}$ and their linear fits obtained for cathodic and anodic peak currents.

Figure 4 (A) depicts the CVs recorded for 4 mM hydroquinone (H_2Q) in 0.1N KNO_3 recorded on bare glassy carbon (GCE, red (b)) glassy carbon modified with glutaraldehyde (GCE-GA, blue (c)) and

Analyst Accepted Manuscript

Ag/Ag_2O-rGO/GCE (green (a)) at scan rate of 100 mV/s. The observed redox peaks in the depicted CVs can be attributed to two-electron redox process of H_2Q.[35] Comparison of the CV recorded on GCE with that recorded on GCE-GA indicates a higher peak current and lesser peak to peak separation (ΔE_p) for the former. For a CV recorded over GCE, while ΔE_p was equal to 286 mV, this parameter increased to 608 mV for the CV recorded over GA-GCE in similar conditions. These changes in the current and potential parameters related to redox behaviour of H_2Q can be attributed to less electro-active nature of GA whose presence on GCE surface hinders the electron transfer. Presence of Ag/Ag_2O-rGO in the glutaraldehyde film was observed to result in significant changes in the current as well as potential characteristics associated with CVs for H_2Q. While on current axes a significant increase in peak currents was observed for both the anodic and cathodic peaks, on the potential axes the gap between these peaks (ΔE_p) was found to be just 98 mV (quasi-reversible) at scan rate of 100 mV/s. A comparison of CVs recorded over Ag/Ag_2O-rGO/GCE (green) with that recorded on GCE (red), and GA-GCE (blue) as depicted in Figure 4(A), clearly indicates that Ag/Ag_2O-rGO electrocatalyses the heterogeneous electron transfer to H_2Q. This can be attributed to superior and efficient electrical conductivity and large surface area of Ag/Ag_2O-rGO/GCE and some inherent and unique structural features of rGO. Additionally, there is a possibility of π-π stacking between rGO and H_2Q which is also expected to facilitate the faradic processes responsible for the observed anodic and cathodic peaks in the recorded CVs (Figure 4(A)). All these features are expected to favour a fast and efficient electron conduction pathway between Ag/Ag_2O-rGO/GCE and H_2Q. Figure 4(B) shows the effect of scan rate on CVs of 4 mM H_2Q in 0.1N KNO_3 recorded on Ag/Ag_2O-rGO/GCE. As clear from the Figure, the peak current of both anodic and cathodic peaks increases and their position on potential axes shows a slight shift with increase in scan rate. The variation of peak current $I_p(a)$ (anodic) and $I_p(c)$ (cathodic) as a function of $\nu^{1/2}$ is depicted as inset of Figure 4 (B). The data follows a linear fit implying that redox behaviour of hydroquinone on Ag/Ag_2O-rGO/GCE is a diffusion controlled process.

Analyst Accepted Manuscript

These above mentioned observations vis-a-vis redox behaviour of H_2Q on the Ag/Ag_2O-rGO/GCE imply that Ag/Ag_2O-rGO composite should exhibit electrocatalytic activity for electro-oxidation of polyhydroxy compounds. In view of the presence of hydroxyl groups in their structure, Ag/Ag_2O-rGO is expected to exhibit excellent electrocatalytic activity for electro-oxidation of biologically important metabolites like ascorbic acid, dopamine, epinephrine, norepinepherine etc. To confirm the same we chose ascorbic acid (AA) as a model molecule to investigate the electrocatalytic and electroanalytic potential of Ag/Ag_2O-rGO/GCE for hydroxyl compounds. Needless to mention, the electrocatalytic behaviour of various electrode materials for AA in neutral media is very important for its selective and sensitive electrochemical detection in real sample solutions.[36] The electrochemical investigations of AA were carried out in 0.1M phosphate buffer of pH 7 as supporting electrolyte.

3.3.Electrochemical behaviour of Ascorbic Acid (AA) on Ag/Ag_2O-rGO/GCE:

The cyclic voltammetric responses of 4 mM Ascorbic acid (AA) in 0.1 M phosphate buffer solution of pH 7 recorded with different electrode systems (blue: baseline, red: GCE and green: Ag/Ag_2O-rGO on GCE) at scan rate of 25 mV/s are shown in Figure 5(A). At bare GCE (red curve), with 4 mM ascorbic acid solution in pH 7 phosphate buffer shows an irreversible oxidation peak at around 0.471 V vs. Ag/AgCl/3M KCl with peak current of ca. 27 μA. However, the redox behaviour of AA is strongly improved on Ag/Ag_2O-rGO/GCE. The characteristic anodic peak of AA is shifted negatively to potential of 3 mV and there is a considerable decrease in its E_p-$E_{p/2}$ value along with significant increase in its peak current. While the E_p-$E_{p/2}$ = 0.139 V was estimated for the CV recorded for AA on the GCE surface, the said value was observed to reduce to 0.039 V for the CV recorded on the Ag/Ag_2O-rGO/GCE in similar conditions. The observed increase in the peak sharpness, peak current and shift in oxidation peak potential corresponding to electro-oxidation of AA on Ag/Ag_2O-rGO/GCE in comparison to that on GCE (468 mV towards more negative) indicates that electro-oxidation of AA on the former is kinetically as well as thermodynamically more facile.

Analyst Accepted Manuscript

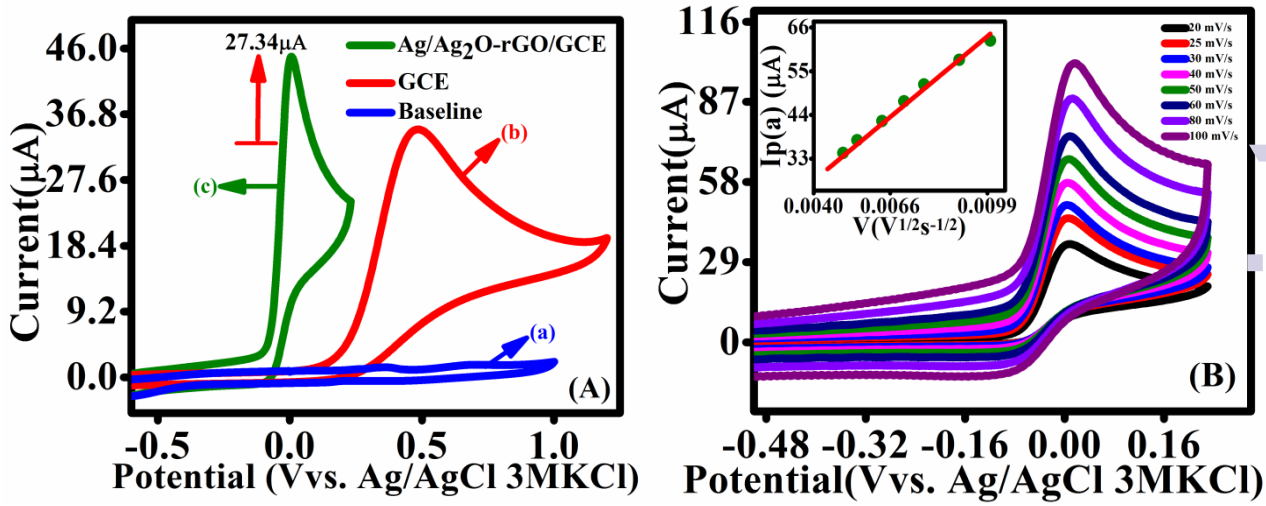

Figure5. (A) CVs recorded (a) on Ag/Ag_2O-rGO/GCE for blank (b) on GCE for 4 mM AA, potential range -1.50 to 1.25 V (c) on Ag/Ag_2O-rGO/GCE for 4 mM AA, potential range -0.90 to 0.20 V, at 298 K in 0.1M phosphate buffer of pH 7 with scan rate of 25 mV/s. (B) CVs recorded on Ag/Ag_2O-rGO/GCE for 4 mM Ascorbic Acid in 0.1M phosphate buffer of pH 7 at 298K on changing scan rates (25-100mV/s). Inset of Figure 5 (B) shows variation between Ip vs. $v^{1/2}$ and linear fit.

These results for electro-oxidation of AA on Ag/Ag_2O-rGO/GCE are in quite contrast to those reported by T-Qi Xu et al for redox behaviour of AA on Pt/rGO-GCE.[37] The suppression of redox behaviour of AA has been also reported on GO modified GCE.[38] Disappearance of electrochemical signal on these modified electrodes has been attributed to inhibition of π-π interactions due to some structural features of composite.[38] The electrocatalytic activity of GO based composites observed for AA in present study is in agreement with that reported by many research groups with other composite materials. A comparison of the results from these reports[39-49] with those observed in this study is presented as Table 1. With oxidation peak of AA positioned at 3 mV vs. Ag/AgCl, 3M KCl and a peak potential shift of 468 mV with respect to GCE, the Ag/Ag_2O-rGO composite synthesised and tested in the present study seems to be a better electro-catalyst for electro-oxidation of AA. This enhanced electrocatalytic activity for AA oxidation on Ag/Ag_2O-rGO/GCE can be attributed to presence of electro-active Ag in various shapes and quinoid like functionalities present on rGO. Figure 5(B) displays the cyclic voltammograms (CVs) of 4 mM AA in 0.1 M phosphate buffer solution of pH 7

Analyst Accepted Manuscript

with different scan rates at Ag/Ag_2O-rGO/GCE. In the investigated range of scan rates, the peak currents shows a linear dependence on the square root of scan rates as depicted in inset of Figure 5(B) which implies a diffusion controlled electro-oxidation of AA over Ag/Ag_2O-rGO/GCE. The absence of reduction peak in reverse scan and positive shift of peak potential with increasing sweep rate (20-100 mV/s), as shown in Figure 5(B) demonstrate that electro-oxidation of AA over Ag/Ag_2O-rGO/GCE is a diffusion controlled, electrochemically irreversible electrochemical process, wherein the heterogeneous electron transfer constitutes the rate determining step.

Electrode System	**pH**	**E_p(bare) (mV)**	**E_p(mod) (mV)**	**Peak potential shift (mV)**	**Scan rate (mV/s)**	**References**
Activated GCE.	7.00 (0.1 M phosphate buffer)	600[a]	270[a]	330	100	[38]
Platinum-Ferrocene.	2.20 (glysine buffer)	-	-	150	50	[40]
Ferrocene-methanol-GCE.	4.00 (glysine buffer)	500[b]	200[b]	300	5	[41]
Ppy/FCN-GCE.	4.00 (glysine buffer)	500[b]	200[b]	300	5	[42]
3,4-dihydroxy benzoic acid Micro disk Au Electrode.	7.00 (phosphate buffer)	380[b]	180[b]	200	10	[43]
Ferrocenecarboxylic acid CPE.	5.00(phosphate buffer)	682[a]	434[a]	248	10	[44]
Plasmapolymerizedvinylpyridine Carbon electrode.	1 M H_2SO_4	760[b]	530[b]	230	100	[45]
1-[4-ferrocenylethynyl]-1-ethan-one carbon paste electrode.	7.00 (phosphate buffer)	591[a]	331[a]	260	10	[46]
Cobalt Pthalocyanine Graphite-epoxy composite electrode.	5.00(phosphate buffer)	320[b]	170[b]	150	20	[47]
SPANI-rGraphene-GCE.	6.8(0.1Mphosphate buffer)	440[b]	100[b]	340	50	[48]
2,7-bis(ferrocenyl ethyl) fluoren-9-one CPE.	5.00(phosphate buffer)	640[a]	340[a]	300	5	[49]
Ag/Ag_2O-rGO/GCE.	**7.00 (0.1Mphosphate buffer)**	**471[c]**	**3[c]**	**468**	**25**	**Present Work**

Table.1 Comparison of efficiency of some modified electrodes towards electrocatalysis of Ascorbic Acid. [a] vs. Ag/AgCl/KCl(sat) [b] vs. saturated calomel electrode [c] vs. Ag/AgCl/ 3M KCl.

The value of $n_a\alpha$ (where n_a is the number of electrons involved in the rate determining step and α is electron transfer coefficient) were calculated for the oxidation of AA at both modified and bare glassy carbon electrodes, using equation 2.[49]

Analyst Accepted Manuscript

$$\alpha n_a = \frac{0.048}{|E_p - E_{p/2}|} \quad (2)$$

The value of αn_a for AA electro-oxidation in 0.1M phosphate buffer of pH 7 on Ag/Ag_2O-rGO/GCE and bare GCE was calculated to be equal to 1.23 and 0.35 respectively. This estimated value of αn_a equal to 1.23 for electro-oxidation of AA on Ag/Ag_2O-rGO/GCE implies that the presence of Ag/Ag_2O-rGO changes the rate determining step from first to second electron transfer step.[39] This change in rate determining step from first to second oxidation step is well supported by sharp increase in peak currents as compared to bare GCE. These observations clearly establish that not only overpotential for ascorbic acid oxidation is reduced at the surface of Ag/Ag_2O-rGO/GCE, but also the rate of electron transfer process is greatly enhanced as confirmed by large I_p(a) values recorded during its cyclic voltammetry.

The electro-catalytic property was studied at changing loading amounts of Ag/Ag_2O-rGO (results not shown) and we found that the electro-catalytic activity happens to be highest for the case when the amount of aqueous dispersion of Ag/Ag_2O-rGO with composition as mentioned in experimental section was kept at 3 μL and the same was used to check the electro-analytic activity of Ag/Ag_2O-rGO.

3.4.Electro analytic performance of Ag/Ag_2O-rGO/GCE:

To assess the electro-analytic performance of Ag/Ag_2O-rGO/GCE, differential pulse voltammetry (DPV) was used as electro-analytic technique because of its high sensitivity and specificity in quantitative analysis. In DPV analysis comparative to CV, the redox peaks are sharper and better defined especially at lower concentrations. In DPV measurements, it was observed that the oxidation peak current corresponding to electro-oxidation of AA at Ag/Ag_2O-rGO/GCE increases with increasing accumulation/deposition time from 0 to 140 s and reached a maximum value for peak current at 140 s. Further increase of accumulation time resulted in almost no change in peak current. The effect of accumulation potential/deposition potential was also investigated. Moreover, DPV

Analyst Accepted Manuscript

analysis can be used to explore the impact of presence of silver as Ag_2O in the Ag/Ag_2O-rGO/GCE. For this, DPV analysis of 4 mM AA in 0.1M phosphate buffer of pH 7 was carried out at changing the deposition potential from 0.0 to -0.8 V, keeping all other accumulation conditions like accumulation time, step potential and modulation amplitude constant. The motivation behind this experiment was to explore the impact of presence of silver in Ag_2O form in the Ag/Ag_2O-rGO/GCE. It is pertinent to mention that electro-deposition of silver has been reported under both cathodic and anodic conditions, however it is reported that the electro-growth rate of silver is more enhanced under cathodic conditions that leads to formation of Ag (0) with better conducting properties.[50]The DPVs recorded for same electro-analyte solution of AA at changing deposition potentials (00 to -0.8 V vs. Ag/AgCl, 3M KCl) are displayed in the form of Figure 6(A). The figure clearly indicates that the redox peak current corresponding to electro-oxidation of AA increase with negative shift of the deposition potential and reaches a maximum value at deposition potential of -0.7 V and then after remains almost constant. Also, with the shift of deposition potential in the negative direction, the redox peak potential shifts towards less positive value, this implies that the electro-oxidation of AA gets facilitated with higher negative deposition potentials. Similar experiments with rGO-GCE do not lead to any appreciable change in the DPVs recorded for AA. On prima facie, the observed changes in the DPVs recorded for AA on Ag/Ag_2O-rGO can be attributed to increased extent of AA deposition with shift of deposition potential in the negative direction. However as already mentioned in the previous section that electro-oxidation of AA at Ag/Ag_2O-rGO/GCE was observed to be a diffusion controlled process, the increase in sensing/analytic behaviour of modified electrode hence should be attributed to the accumulation of more and more silver nanoparticles which result from electro-reduction of Ag_2O in the Ag/Ag_2O-rGO composite when held at more negative potentials. This newly accumulated silver species on the electrode surface improves the charge transferability of Ag/Ag_2O-rGO to AA. Therefore, increase in peak currents and shift of peak potential towards less positive potentials with increasingly negative deposition potentials in DPV measurements can be attributed to presence of Ag_2O in the Ag/Ag_2O-rGO, which in turn get reduced during the electro-deposition process. These cited observations clearly

Analyst Accepted Manuscript

establish that for Ag/Ag_2O-rGO composite the presence of oxide form of silver reduces its electro-analytic and electro-catalytic performance for AA.

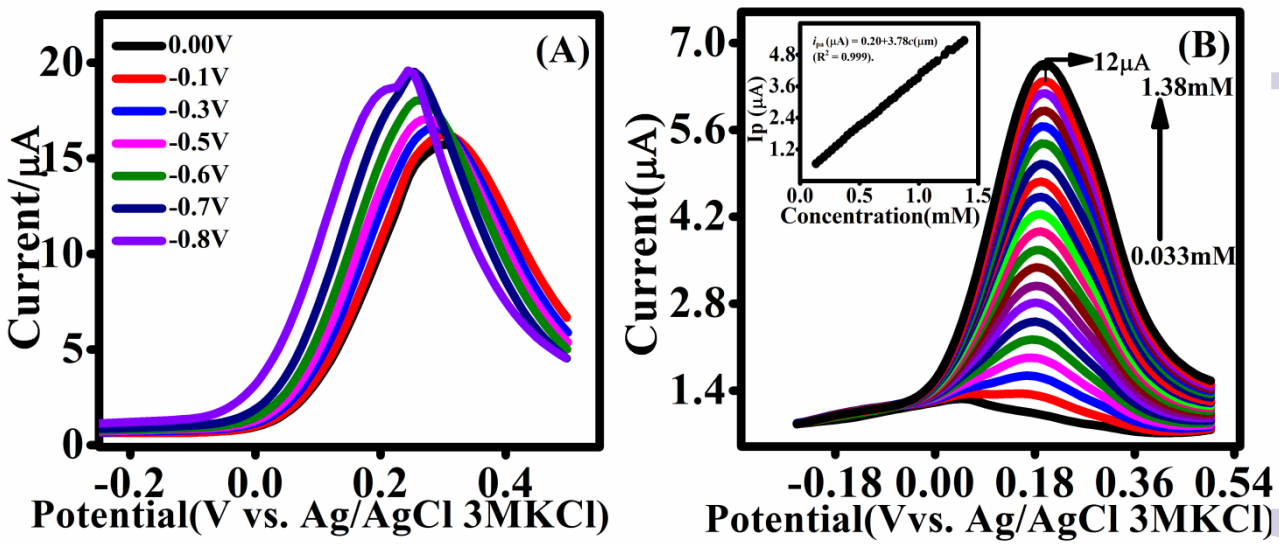

Figure6. (A) DPVs recorded for 4 mM ascorbic acid in 0.1M Phosphate Buffer of pH 7 at 298 K on Ag/Ag_2O-rGO/GCE at changing deposition potentials. (B) DPVs recorded for changing concentrations of ascorbic acid in 0.1M phosphate buffer of pH 7 at 298 K on Ag/Ag_2O-rGO/GCE (Deposition potential = -0.7 V, Deposition time = 140 s, Modulation amplitude = 0.05 V). (Inset graph of 6(b) depicts calibration plot between Ip vs. Concentration (mM) of ascorbic acid with linear behaviour in concentration range of 0.033-1.38 mM, R^2= 0.999).

Therefore, the parameters optimised for electro-analysis of AA through DPV were, deposition potential equal to -0.7 V, deposition time 140 s, scanning the potential range from -0.25 to 0.50 volts vs. Ag/AgCl (3M KCl), differential pulse step potential of 0.009 V and modulation amplitude of 0.05 V. With these optimised parameters, DPVs in 0.1 M phosphate buffer of pH 7 across Ag/Ag_2O-rGO/GCE with changing amounts of AA were recorded. The DPVs recorded as such for changing concentrations of AA in 0.1M phosphate buffer are displayed in the form of Figure 6(B). As evident the redox peak current corresponding to electro-oxidation of AA increases with increase in the amount of AA in the electro-analyte solution. The observed redox peak currents when plotted as a function of concentration of AA exhibited a linear increase with the increase in concentration of AA and the same is depicted as inset in Figure 6(b). The data depicted in inset of Figure 6(B) was observed to follow a linear equation i_{pa}(μA) =

Analyst Accepted Manuscript

0.20 + 3.78c(μm) (R^2 = 0.999) in the investigated concentration range. The normalized sensitivity $\bar{\iota}_p$($AS^{1/2}/V^{1/2}Mcm^2$) of the Ag/Ag_2O-rGO/GCE was estimated through equation 3: [51]

$$\bar{\iota}_p = \frac{i_p}{nAv^{1/2}C_o} \quad (3)$$

where n is number of electrons involved in oxidation/reduction process of electro-analytes which in case of ascorbic acid is reported to be equal to 2, i_p is anodic peak current, A is electroactive area of modified electrode, v is scan rate and C_o is bulk concentration. At scan rate of 0.025 V/s and concentration of 4 mM AA, the normalized sensitivity $\bar{\iota}_p$of 7.9 $AS^{1/2}/V^{1/2}Mcm^2$ was estimated**.** From the slope of calibration plot and electroactive area A, the sensitivity of the modified electrode was found to be equal to 0.087 $AM^{-1}cm^{-2}$ or 3.8 μA/μM. In comparison to previously reported electrodes like AgNPs/rGO[21] with sensitivity 0.45 μA/μM and electrochemically reduced graphene oxide (ERGO)[52] with sensitivity of 0.5 μA/mM, the Ag/Ag_2O-rGO/GCE used in present study seems to display better sensitivity towards detection of AA.

4. Conclusion:

We have demonstrated a simple electrochemical approach to establish the presence of silver oxides in Ag-graphene nano composites synthesised under alkaline conditions. The nanocomposites comprise of nanodimensional Ag_2O@Ag well dispersed on rGO and show excellent electrocatalytic and electrosensing activity for electro-oxidation of AA. The activity of the composite being affected by the extent of silver oxide whose electroreduction results in the enhancement of the electrochemical performance of the Ag/Ag_2O-rGO nanocomposite for AA electrooxidation. Complete electroreduction of oxide phase of silver in Ag/Ag2O-rGO composites leads to sensitivity of 0.087 $AM^{-1}cm^{-2}$ or 3.8 μA/μM which is better than most of the materials that have been so far tested for electrooxidation of AA.

Analyst Accepted Manuscript

5. Acknowledgements

MAB thanks Department of Science and Technology, New Delhi, India, for the research grant No. SR/S1/PC-11/2009. SAB thanks DST for the financial assistance under DST INSPIRE scheme. MAR thanks CSIR for financial assistance.

References:

1. V. Georgakilas, M. Otyepka, A. B. Bourlinos, V. Chandra, N. Kim, K. C. Kemp, P. Hobza, R. Zboril, and K. S. Kim, *Chem. Rev.*, 2012**, 112**, 6156-6053.
2. M. Liu, R. Zhang, and W. Chen, *Chem. Rev.*, 2014, **114**, 5117-5160.
3. A. Chen and P. Holt-Hindle, *Chem. Rev*., 2010**, 110**, 3767–3804.
4. A. Kongkanand and P. V. Kamat, *J. Phys. Chem. C*, 2007, **111**, 9012-9015.
5. G. Williams, B. Seger and P.V. Kamant. *ACS NANO*, 2008, **2**, 1487-1491.
6. X. Feng, Y. Zhang, J. Song, N. Chen, J. Zhou, Z. Huang, Y. Ma, L. Zhang, and L. Wang, *Electroanalysis*, 2014, **26**, 1-8.
7. L. Tammeveski, H. Erikson, A. Sarapuu, J. Kozlova, P. Ritslaid,V. Sammelselg and K. Tammeveski, *Electrochemistry Communications*, 2012, **20**, 15-18.
8. K. M. Samant, V. S. Joshi, G. Sharma, S. Kapoor and S. K. Haram, *Electrochimica Acta*, 2011, **56** 2081–2086.
9. A. Devadoss, P. Sudhagar, S. Das, S. Y. Lee, C. Terashima, K. Nakata, A. Fujishima, W. Choi, Y. S. Kangand U. Paik, *ACS Appl. Mater. Interfaces*, 2014, **6**, 4864-4871.
10. Q. Xiang and J. Yu, *J. Phys. Chem. Lett.*, 2013, **4**, 753-759.
11. P. V. Kamat, *J. Phys. Chem. Lett*., 2010, **1**, 520-527.
12. Q. Zhuo, Y. Ma, J. Gao, P. Zhang, Y. Xia, Y. Tian, X. Sun, J. Zhong and X. Sun, *Inorg. Chem.*, 2013, **52**, 3141-3147.
13. X. Chen, G. Wu, J. Chen, X. Chen, Z. Xie, and X. Wang, *J. Am. Chem. Soc.*, 2011, **133**, 3693-3695.

Analyst Accepted Manuscript

14. R. Kou, Y. Shao , D. Wang, M. H. Engelhard, J. H. Kwak , J. Wang, V. V. Viswanathan, C. Wang, Y. Lin , Y. Wang, I. A. Aksay and J. Liu, *Electrochemistry Communications*, 2009, **11**, 954-957.

15. S. Dutta, C. Ray, S. Sarkar, M. Pradhan, Y. Negishi, and T. Pal, *ACS Appl. Mater. Interfaces*, 2013, **5**, 8724-8732.

16. A. Ehsani, B. Jaleh and M. Nasrollahzadeh, *Journal of Power Sources*, 2014, **257**, 300-307.

17. E. J. Lim, S. M. Choi, M. H. Seo, Y. Kim, S. Lee and W. B. Kim, *Electrochemistry Communications*, 2013, **28**, 100-103.

18. X. Qin, Y. Luo, W. Lu, G. Chang, A. M. Asiri, A. O. Al-Youbi and X. Sun, *Electrochimica Acta*, 2012, **79**, 46-51.

19. J. Geng, Y. Bi and G. Lu, *Electrochemistry Communications*, 2009, **11**, 1255-1258.

20. N. Wang, X. Cao, Q. Chen, and G, Lin, *Chem. Eur. J.*2012, **18**, 6049– 6054.

21. V. Bansal, V. Li, A. P. O'Mullane and S. K. Bhargava, *CrystEngComm*, 2010, **12**, 4280-4286.

22. J. Tian, S. Liu, Y. Zhang, H. Li, L. Wang, Y. Luo, A. M. Asiri, A. O. Al-Youbi, and X. Sun, *Inorg. Chem.*, 2012, **51**, 4742-4746.

23. B. Kaur, T. Pandiyan, B. Satpati and R. Srivastava, *Colloids and Surfaces B: Biointerfaces*, 2013, **111**, 97-106.

24. R. Pasricha, S. Gupta and A. K. Srivastava, *Small*, 2009, **5**, 2253-2259.

25. B. X. Fan, W. Peng, Y. Li, X. Li, S. Wang, G. Zhang, and F. Zhang, *Adv. Mater.*, 2008, **20**, 4490-4493.

26. M. A. Macchione, O. A. Douglas-Gallardo, L. A. Pérez, N. Passarelli, R. Moiraghi, A. Spitale, D. Bahena, F. Y. Oliva, M. M. Mariscal, M. José-Yacamán, E. A. Coronado, V. A. Macagno and M. A. Pérez, *Journal of Colloid and Interface Science*, 2014, **428**, 32-35.

27. A. F. Benton and L. C. Drake, *J. Am. Chem. Soc.*, 1934, **56**, 255-263.

28. P. J. Herley and E. G. Prout, *J. Am. Chem. Soc.*, 1960, **82**, 1540-1543.

29. D.C. Marcano, D. V. Kosynkin, J. M. Berlin, A. Sinitskii, Z. Sun, A. Slesarev, L. B. Alemany, W. Lu, and J. M. Tour, *ACS NANO*, 2010, **4**, 4806-4814.

Analyst Accepted Manuscript

30. M. A. Bhat, P. P. Ingole, V. R. Chaudhari and S. K. Haram, *New J. Chem*., 2009, **33**, 207-210.

31. G. Y. Kim, N. M. Cuong, S. H. Cho, J. Shim, J. J. Woo and S.H. Moon, *Talanta*, 2007**, 71**, 129-135.

32. O. A. D. Gallardo, R. Moiraghi, M. A. Macchione, J. A. Godoy, M. A. Pe´rez, E. A. Coronado and V. A. Macagno, *RSC Adv*., 2012, **2**, 2923-2929.

33. J. Ghilane, F.F. Fan and A.J. Bard, *Nano Lett.*, 2007, **07**, 1406-1412.

34. R.S. Nicholson and I. Shain, *Anal Chem*, 1964, **36**, 706-723.

35. M. A. Bhat, *Electrochimica Acta*, 2012, **81**, 275– 282.

36. A. Malinauskas, R. Garjonyt˙e, R. Mažeikien˙e, and I. Jurev ci¯ut˙e, *Talanta*, 2004, **64**, 121-129.

37. T. Xua, Q. Zhanga, J. N. Zheng, Z. Lv, J. Weia and A. Wang, J. Feng, *Electrochimica Acta***,** 2014 **115**, 109-115.

38. F. Gao, X. Cai, X. Wang, C. Gao, S. Liu, F. Gao and Q. Wang, *Sensors and Actuators B*, 2013, **186**, 380-387.

39. I. F. Hu and T. Kuwana, *Anal chem.*, 1986, **58**, 3235-3239.

40. M. Peterson, *Anal. Chim. Acta*, 1986,**187**, 1333-1343.

41. R. Ojani and M. H. Pournaghi-Azar**,** *Talanta*, 1995, **42**, 1839-1848.

42. M. H. Pournaghi-Azar and R. Ojani, *J. Solid State Electrochem*. 2000, **4**, 75-79.

43. J.J. Sun, D.M. Zhou, H.Q. Fang and H.Y. Chen, *Talanta*, 1998, **45**, 851-856.

44. R. Ojani, J. B. Raoof and S. Zamani, *Electroanalysis*, 2005, **17**, 1740-1745.

45. R. W. Murray and J. Facci, *Anal. Chem.*1982, **54**, 769-772.

46. M. H. Pournaghi-Azar and H. Razmi-Nerbin, *J. Electroanal. Chem.*, 2000, **488**, 17-24.

47. S. A. Wring, J. P. Hart and B. J. Brich, *Anal. Chim. Acta*, 1990, **229**, 63-70.

48. H. Bai, Y. Xu, L. Zhao, C. Li and G. Shi, *Chem. Commun*., 2009, **233**, 1667-1669.

49. J. B. Raoof, R. Ojani, H. Beitollahi and R. Hossienzadeh, *Electroanalysis*, 2006, **18**, 1193-1201.

50. I. G. Casellaand M. Ritorti, *Electrochimica Acta*, 2010, **55**, 6462-6468.

51. D. Kim, I. B. Goldberg and J. W. Judy, *Analyst*, 2007, **132**, 350-357.

Analyst Accepted Manuscript

52. L. Yang, D. Liu, J. Huang and T. You, *Sensors and Actuators B*, 2014, **193**, 166-172.

Analyst Accepted Manuscript